COMPARATIVE ANALYSIS OF THE RIGOROUS AND THE POLYNOMIAL FUNCTION MODELS FOR THE CARTOGRAPHIC ACCURACY ASSESSMENT OF IKONOS ORTHOIMAGES AND DSMs

Análise Comparativa entre o Modelo Rigoroso e o Modelo de Função Polinomial na Determinação de Precisão Cartográfica de Ortoimagens e MDSs IKONOS

Lívia Rodrigues Tomás[1]
Cláudia Maria de Almeida[2]
Cleber Gonzales de Oliveira[3]
Leila Maria Garcia Fonseca[4]

National Institute for Space Research - INPE
Division for Remote Sensing (DSR) – Division for Images Processing (DPI)
Av. dos Astronautas, 1758 – 12227-010 São José dos Campos, SP
[1]lívia@dsr.inpe.br
[2]almeida@dsr.inpe.br
[3]cleber@dsr.inpe.br
[4]leila@dpi.inpe.br

ABSTRACT

Digital terrain models have made the earth surface modelling available. With the use of interpolated samples and depending on their location, different digital models can be created. Digital elevation models (DEMs) are built upon basis of samples referring to points located on the terrain, while digital surface models (DSMs) account for the elevation of natural and artificial features located above ground. The sources for the acquisition of elevation data are manifold, and the selection of the most appropriate ones for a given study will always rely on the specific goals at issue. In this paper, a 1m stereo pair of IKONOS-2 images covering part of Mairiporã municipality, São Paulo State, was used. This article is firstly committed to evaluate the elevation accuracy of DSMs obtained from a stereo pair of IKONOS images and their rational polynomial coefficients (RPC), with different combinations of ground control points (GCPs), and secondly, to assess the planimetric (positional) accuracy of orthoimages generated from DSMs with better elevation accuracy. The DSMs were generated with five different sets of GCPs: 9, 12, 15, 18, and 21. Each DSM and orthoimage were evaluated based on the root mean square error, using 21 independent check points (ICPs) surveyed on field. The RPC method, which allows the generation of relative DEMs and is less dependent on GCPs, yielded better accuracy than Toutin´s model both in the orthoimages and in the DEMs and DSMs generation.

Keywords: Remote Sensing, Digital Surface Model, Stereoscopy, Accuracy Assessment.

RESUMO

Através das técnicas de modelagem digital do terreno, é possível modelar a superfície terrestre através de amostras. Essas amostras, após serem interpoladas, e de acordo com a localização, dão origem a diferentes tipos de modelos digitais. Quando a elevação da grade provém apenas de pontos localizados na superfície nua do terreno, tem-se um modelo digital de elevação; quando incorpora valores de elevação das feições naturais e artificiais situadas acima da superfície nua do terreno, tem-se um modelo digital de superfície. Neste trabalho, foram utilizadas imagens estereoscópicas do sensor a bordo do satélite IKONOS-2, com 1 metro de resolução espacial, que recobrem parte do município de Mairiporã – SP. O objetivo deste trabalho é avaliar a acurácia vertical de modelos digitais de superfície, gerados a partir de um par estereoscópico de imagens IKONOS e respectivos coeficientes polinomiais racionais (*RPC*), e a acurácia posicional de ortoimagens geradas a partir dos modelos digitais de superfície com maior acurácia vertical. Os modelos digitais de superfície foram gerados com cinco diferentes combinações de pontos de controle: 9, 12, 15, 18 e 21. Cada modelo e ortoimagem foram avaliados através do erro médio quadrático, com base em 21 pontos de validação levantados em campo. A modelagem *RPC* apresentou maior acurácia em relação à de Toutin na geração dos modelos e ortoimagem, e ainda apresenta vantagens como possibilidade de geração de modelos relativos e menor dependência do uso de pontos de controle.

Palavras chaves: Sensoriamento Remoto, Modelo Digital de Superfície, Estereoscopia, Avaliação de Acurácia.

1. INTRODUCTION

The new techniques used for generating digital elevation models enabled the modelling of continuous surfaces in a discrete form with the aid of samples. These samples (elevation points with spatial coordinates) are interpolated to obtain either a triangular or a regular network. A numerical grid regularly spaced (in X and Y), with elevation values (Z), geocoded to a datum (horizontal and vertical) and to a cartographic projection system yields a specific digital elevation model (DEM). When the grid elevation values refer to points located on the terrain surface, we have a digital terrain model (DTM); when they include elevation values of both terrain surface and natural or man-made features located above ground, we have a digital surface model (DSM) (MAUNE et al., 2007).

The elevation data can be obtained by means of GPS/DGPS points collection in the field, a stereo pair of aerial photos, a stereo pair of orbital sensor images, laser scanning, interpherometry, and radargrammetry. The type of data acquisition should take into account the study goal, the envisaged level of detailing (scale), and the available financial resources. The obtained models, DTM or DSM, can be used in several applications, like orthorectification of satellite imagery, hydrological and geomorphological studies, meteorological and climatic investigations and simulations, forest resources assessment, natural or man-made hazards prevention, agricultural, environmental, and urban planning and management, among others.

In this work, a stereo pair of high spatial resolution images, acquired by a sensor on-board of IKONOS-2 satellite, and ground control points − GCPs collected in the field with a single frequency geodetic GPS equipment, were used in the generation of DSMs for the area covered by the images stereo pair. This stereo pair enables the extraction of a three-dimensional surface model, which technique is known as stereoscopy. The main goal of stereoscopy is to reconstruct a three-dimensional space (object-space) from a set of bi-dimensional images (image-space) (BRITO & COELHO, 2002). The choice of a given stereoscopic procedure will have an influence not only on the resulting three-dimensional models accuracy, but also on the accuracy of by-products derived from such models. In this way, numerous works in the scientific literature nowadays have been devoted to create and/or explore methods to assess the planimetric (positional) and elevation accuracy of digital terrain and digital surface models as well as of orthoimages generated by such models (KYRIAKIDIS et al., 1999; GRODECKI & DIAL, 2001; CHENG et al., 2003; BÜYÜKSALÍH et al., 2004; TOUTIN, 2004a; WOLNIEWICZ & JASZCZAK, 2004; CAMARGO et al., 2008; CHENG et al., 2008; HARRY et al., 2008; YILMAZ et al., 2008; LI et al., 2009).

Specifically concerning IKONOS imagery, AGUILAR et al. (2007) evaluated the performance of four models using the root mean square error (RMSE), in order to identify the one that would result in the best positional accuracy for orthorectified images. The selected models were: i) 3D first-order rational functions, without the ancillary data provided by the images vendor, ii) 3D rational functions refined by the user with a zero-order polynomial fit, iii) 3D rational functions refined by the user with a first-order polynomial fit, and iv) physical or rigorous model, also known as Toutin´s model (TOUTIN & CHENG, 2000). The authors used 60 sets of GCPs, 30 of which with 9 GCPs and the remaining 30 with 18 GCPs. They concluded that the best result was obtained by the model with a zero-order polynomial fit and that a number of GCPs superior to nine did not improve the results obtained by the winner model. On the other hand, CHENG & TOUTIN (2001) committed themselves to assess the elevation accuracy of IKONOS and EROS-A1DEMs and the positional accuracy of orthoimages derived from such DEMs using a simple polynomial model (which does not consider the elevation information and is restricted to small flat areas), the rational polynomial model or RPC (OGC, 1999), and the physical or rigorous model (TOUTIN & CHENG, 2000). In the three cases and for both satellites, 30 GCPs were used, or 7 GCPs and 23 validation points (independent check points − ICPs) otherwise. The authors came to the conclusion that, in a general way, the smallest errors were obtained by the rigorous model, which proved to be stable, robust, and able to meet cartographic standards required at a 1:4 800 scale.

A similar work using the last two methods (RPC and rigorous) exclusively for IKONOS images was done by DAVIS & WANG (2001). The authors assessed the accuracy of images orthorectified with DEMs supplied by the United States Geological Survey (USGS) and concluded that the use of a DEM with the highest resolution as possible is always advisable, particularly in urban areas, where it is necessary to preserve the positional accuracy of neighbouring features with considerably different elevations (e.g. buildings and roads). For the authors, the elevation accuracy of DEMs extracted by means of stereo correlation always worsens as the spatial resolution increases, what in turn negatively impacts the positional accuracy and visual quality of orthoimages derived from such models. Smaller viewing angles would be as well more appropriate for the generation of high accuracy orthoimages, since the horizontal pixels shift caused by topographic variations and the thereof resulting DEM errors would be minimised. The authors also acknowledged that the rigorous model presents the advantage of requiring a reduced number of GCPs to generate a worthy model for the entire scene. The RPC model, on the other hand, is able to correct positional distortions only in the surroundings of GCPs and is thus appropriate for small areas, relatively flat, and with a considerable number of GCPs.

PEDRO *et al.* (2007) conducted a comparative analysis on the performance of the RPC model and the affine projection model (APM) for the purpose of orthorectifying IKONOS and QuickBird images. In the first case (RPC), the authors used 24 and 13 GCPs for IKONOS and QuickBird images, respectively. In the second case (APM), 24 and 15 GCPs were respectively used. The APM transformation model proved to be suuperior, for it is able to model the existing distortions in both images, offers better positional quality, does not present systematic trends in the orthoimages residuals, besides being applicable to images of reduced size. The authors concluded that the type of pre-processing (pan-sharpening or resampling) and the characteristics of the image acquisition (Forward, Reverse, Nadir) have an impact on the orthorectification model performance, since these premises influence not only the visual quality but also the positional quality, as they are closely related to the images generation. In the same line of investigation, ARAÚJO *et al.* (2008) evaluated the RPC and the rigorous models for the orthorectification of a QuickBird image, using 30 GCPs. The authors observed that rigorous methods should be used in images acquired with high side-viewing angles and/or related to regions with great variations in elevation, for they reconstruct the sensor physical geometry. According to them, although the RPC model is less accurate than the rigorous one, the conducted tests revealed the efficiency of the former one when ground control points and a refined DTM were used.

Some authors customised conventional methods in order to assess the accuracy of high spatial resolution products for specific applications. WOLNIEWICZ & JASZCZAK (2004) assessed the positional error of IKONOS and QuickBird orthoimages, aiming to identify the true position of buildings. The authors used the RPC and the rigorous model (TOUTIN & CHENG, 2000) for orthorectifying the images with a constant number of 9 GCPs, though combined with different number of validation points (ICPs), namely 18, 30 and 92. According to them, the best results are in general obtained by the rigorous model. However, this model requires a minimum number of GCPs that varies as a fuction of the type of terrain, whereas the RPC model reaches a slightly inferior accuracy regardless of the number of GCPs. For them, the type of terrain (flat or steep) and the type of DEM used define the orthorectification accuracy, although the most important premise would be to assure a high accuracy in the identification, interpretation, and collection of control points both in the field and in the image.

DI *et al.* (2003) assessed the accuracy of IKONOS orthorectified images for the purpose of coastal mapping. The authors used the coefficients of a rational function (RF), supplied by the images vendor, in order to evaluate the nominal accuracy of points on the terrain in relation to control points. A substantial improvement in the accuracy was obtained by applying a 3D affine transformation function to the 3D terrain points, calculated by the rational function and aimed at correcting systematic errors. The positional and elevation accuracies of the DEM and the orthoimages were assessed by the ICPs. VASSILOPOULOU *et al.* (2002), on their turn, evaluated the positional error of an IKONOS DEM and orthoimages used for monitoring a volcanic eruption in the Greek island of Nisyros. Likewise the preceding work the authors applied transformations aiming to increase the orthorectification accuracy. Two methods were employed to achieve this goal: an affine transformation with relief correction and also with Kratky´s polynomial mapping functions. The orthorectification accuracy was then evaluated by means of GCPs employed as validaton points. Another work in the same line of research was done by BALTSAVIAS *et al.* (2001), who conducted a geometric evaluation of geocoded IKONOS images that would be further used for a three-dimensional modelling of buildings. The RPC model with 28 GCPs was used for orthorectifying the images. The authors demonstrated that with a reduced number of accurate and well distributed GCPs, it is possible to substantially increase the positional and elevation accuracy, maintaining 60 coefficients on average per image. In the same way, the authors showed that it is possible to obtain a similar accuracy using a 2D affine transformation with relief correction, or a 3D affine transformation otherwise, both with only 3 GCPs.

In a totally diverse approach in relation to the ones previously presented, this work is committed to assess the elevation accuracy of DSMs extracted from an IKONOS-2 stereo pair and the positional accuracy of orthoimages derived from such DSMs using the RPC and the rigorous model, but with the particularity of adopting variable settings of GCPs. The obtained results are evaluated and classified acordding to the Brazilian Cartographic Accuracy Standard, know as *PEC* (*Padrão de Exatidão Cartográfico*). The DSMs with the highest elevation accuracy generated by each of the two models will then be further used to orthorectify one of the stereo pair images (the one that is closest to Nadir). The orthoimages will be as well evaluated and classified according to *PEC*.

2. MATHEMATICAL MODELS

According to TOUTIN (2006), two 3D mathematical models, physical and empiric, are usually used for stereoscopic processing and extraction of DSMs from high spatial resolution images (IKONOS and QuickBird, mainly). Examples of physical and empiric models are the one developed by Toutin at the Canada Centre for Remote Sensing (CCRS), and the rational function model (RFM), respectively.

Toutin´s model is embodied in the software OrthoEngine of PCI Geomatics. This 3D physical model is applied to multisensor images and is regarded as robust and not sensitive to the GCPs distribution, provided there is no positional or elevation extrapolation. This mathematical modelling represents the colinearity and coplanarity conditions for stereo

models, integrating different distortions related to the images acquisition geometry. They may refer to distortions related to the satellite, to the sensor itself, to the Earth rotation or to deformations resulting from the cartographic projection (TOUTIN; 2004b; 2006). Further details on this modelling using IKONOS images are found in TOUTIN (2003).

The RFM is on its turn based on a ratio of polynomial functions (equation (1)), and its implementation procedures are two-fold: (i) the model is exclusively solved based on parameters of a third-order rational polynomial provided for each image by the respective vendor, and (ii) the model employs ground control points acquired or supplied by the images end user, which will then define the order of the polynomial functions that will be used. The first approach is inappropriately called "*terrain-independent*", and the second one is called "*terrain-dependent*" (TOUTIN, 2006). The first approach (i) is also known as rational polynomial coefficients (RPC) method.

$$R_{3D}(XYZ) = \frac{\sum\limits_{i=0}^{m}\sum\limits_{j=0}^{n}\sum\limits_{k=0}^{p} a_{ijk} X^i Y^j Z^k}{\sum\limits_{i=0}^{m}\sum\limits_{j=0}^{n}\sum\limits_{k=0}^{p} b_{ijk} X^i Y^j Z^k} \quad , \qquad (1)$$

where:
X, Y, Z are the terrain or cartographic coordinates;
i, j, k are integer increments;
m, n e p are integer values; and
$m+n+p$ is the order of the polynomial function.

It is worth mentioning that the processing steps for generating a DSM in OrthoEngine are practically the same for both modelling approaches (Toutin and RFM). The main steps are presented below (Figure 1).
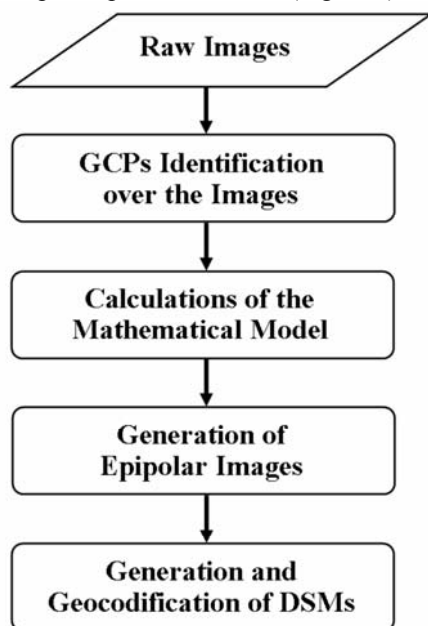

Fig. 1 - Main steps for generating a DSM.

3. MATERIAL AND METHODS

The study area is located in the municipality of Mairiporã (SP) and is contained with a bounding box with the following coordinates: 46º 38' 06" W; 23º 19' 45" S; e 46º 33' 03" W; 23º 17' 22" S (Figure 2).

The material employed in this work consist of: 1) 42 ground control points collected in the field in October of 2007 with a single frequency geodetic GPS equipment, operated in the relative positioning static mode; and 2) a stereo pair of IKONOS-2 images, with 1 m of spatial resolution. The IKONOS-2 stereoscopic images were available in two types of positional accuracy level: Reference and Precision, with 1 m of spatial resolution (pan-sharpened) and 11 bits of radiometric resolution.

The images stereo pair is acquired in the same orbital passage, with just a few seconds of difference, what makes the further process of identifying homologous features in the images much easier. Together with the images, the rational polynomial coefficients − RPCs of each image are as well provided, which account for the relation between the object-space and the image-space. The geometric accuracy of the stereo images depends on the use of GCPs, as shown in Table 1. Table 2 and Figure 3 present the IKONOS-2 images acquisition geometry. The multispectral bands were pan-sharpened with the panchromatic band using the *GranSchmidt* method (LABEN & BROWER, 2000).

TABLE 1 - GEOMETRIC ACCURACY OF IKONOS-2 STEREOSCOPIC PRODUCTS.

Product	Horizontal Accuracy CE90*	Vertical Accuracy LE90**
Stereo pair with no GCPs	25 m	22 m
Stereo pair with GCPs	2 m	3 m

Source: Dial (2000).

*The circular error (CE90) is a measure of positional errors of a given cartographic product combined in latitude and longitude, with no regard to the elevation accuracy. It concerns a circular radius (given in meters) comprising 90% of all positional errors of the product under analysis in relation to the true coordinates on the ground (PARADELLA *et al.*, 2005).

**The linear error (LE90) is world-wide used to quantify the elevation error of a DSM in relation to the real elevation values (true elevation) with a confidence interval of 90% (PARADELLA *et al.*, 2005).

TABLE 2 - IMAGES TECHNICAL SETTINGS.

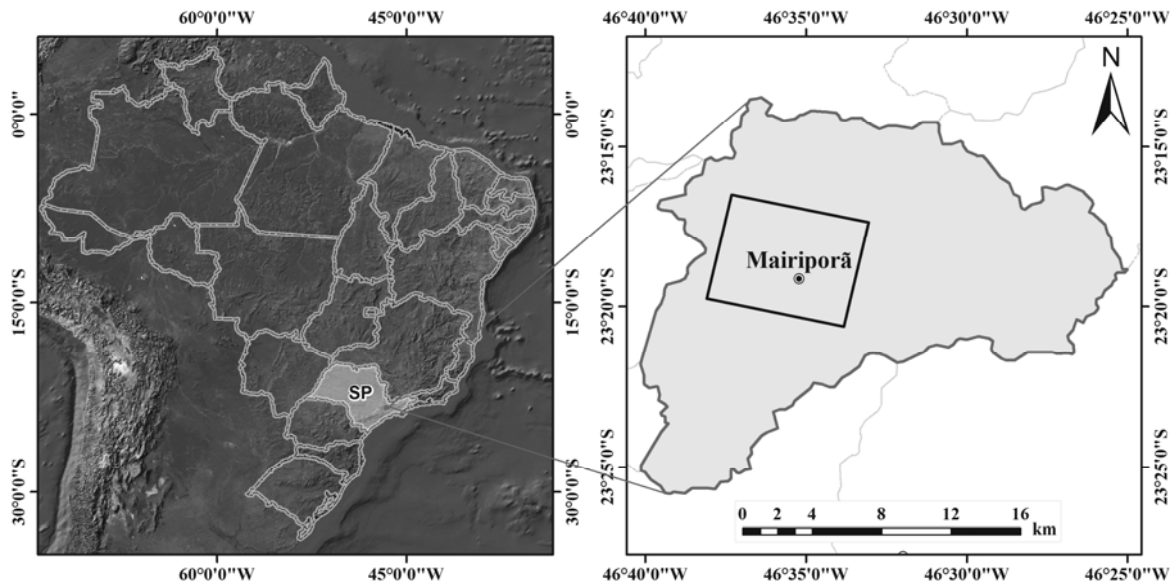| IKONOS-2 Images	0030020100	0020030100
Acquisition Date	09/07/2000	09/07/2000
Stereo Positioning	left	right
Sensor Elevation Angle (1)	88.48º	60.44º
Sensor Azimuth Angle (2)	240.95º	10.47º
Sun Azimuth Angle (3)	36.58º	36.77º
Sun Elevation Angle (4)	34.93º	34.81º

Fig. 2 - Location of study area.

The methodology employed in this work can be summarised in the following steps:

a) planning of the field work;
b) field work accomplishment;
c) processing and evaluation of the GPS points collected in the field with a geodetic GPS equipment;
d) collection of control points and validation on the stereo pair of IKONOS-2 images;
e) generation of the DSMs;
f) statistical evaluation of the DSMs;
g) generation of two orthoimages from the two DSMs with the best statistical results;
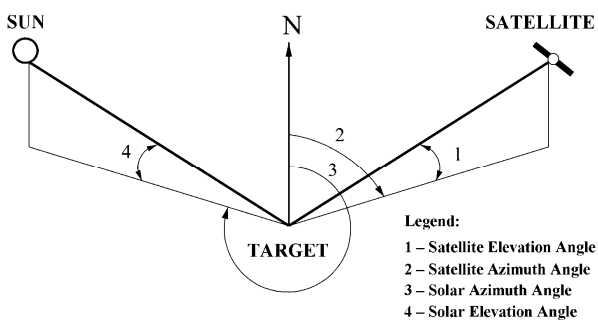h) statistical evaluation of the orthoimages.

Fig. 3 - IKONOS images acquisition geometry.
Source: GRODECKI & DIAL (2001).

The field work planning was based on the IKONOS-2 images, on which remarkable features regularly scattered over the stereo pair coverage area were selected as potential points to be collected in the field.

A total of 42 points were collected in the field, and half of them (21 points) were reserved for validation. According to MERCHANT (1982), a minimum of 20 points should be used for validation. In this way, the remaining 21 points were used in the generation of the DSMs.

Initially, a minimum of 9 GCPs was used to generate the first DSMs, which were spatially scattered throughout the study area and representative of the different elevation values found in such area. Since the maximum number of GCPs was set to 21, we decided to adopt five different settings of GCPs (9, 12, 15, 18, and 21) to generate the DSMs. Figure 4 shows the location of GCPs in the study area.

The control points were inserted on both images of the stereo pair, taking into account information obtained during the field work and following the previously defined GCPs settings.

In an effort to reduce the positional error and to increase the correlation of homologous features, tie points (TPs) were collected on both images. It is worth mentioning that the software PCI Geomatica OrthoEngine – release 9.0, which was used in this work, does not allow the insertion of TPs in the RPC model. Therefore, only GCPs were used in such model, resulting in the generation of 5 DSMs according to the settings presented in Figure 4.

In Toutin´s model, the insertion of TPs significantly increased the residuals estimation. Hence, 5 DSMs with no TPs and other 5 DSMs with TPs were generated, so as to allow an accuracy comparison of such products regarding the inclusion or exclusion of TPs.

Considering that the RPC model allows the generation of a relative DSM (with no GCPs), and that

the insertion of TPs was not possible, an additional DSM with no GCPs was generated.
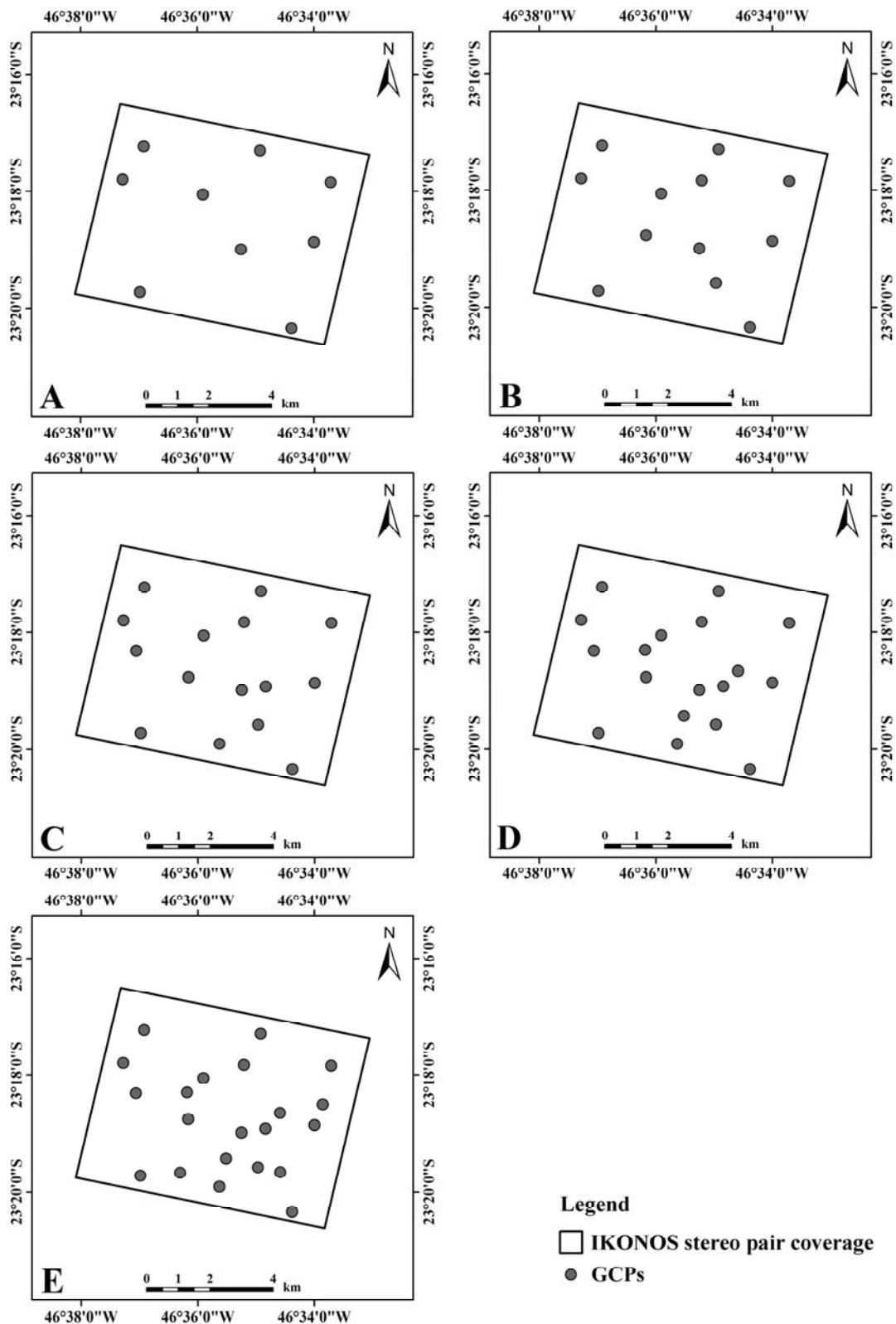

Fig. 4 - Location of the sets of (A) 9 GCPs; (B) 12 GCPs; (C) 15 GCPs; (D) 18 GCPs; and (E) 21 GCPs in the study area, used in the generation of the DSMs.

A total of 16 DSMs were generated; one of which was a relative model. The remaining 15 DSMs observed the same settings of GCPs, 5 with the RPC

model, and 10 with Toutin´s model (5 DSMs with no TPs and 5 with TPs).

After this step, the calculations of the mathematical model for the generation of epipolar images and generation and geocoding of the 16 DSMs with 8 m of spatial resolution were finally accomplished.

Finally, the accuracy assessment of each DSM and of the two orthoimages was executed based on the 21 ICPs, shown in Figure 5. The elevation discrepancies h of a given poin i in the DSMs as well as the positional discrepancy of a given point i in the orthoimages are calculated based on the UTM coordinates (E, N) of each ICP, according to the following equations:

$$\Delta h_i = h_i^r - h_i^c \quad, \tag{2}$$

$$\Delta E_i = E_i^r - E_i^c \quad, \tag{3}$$

$$\Delta N_i = N_i^r - N_i^c \quad, \tag{4}$$

where h is the elevation, E and N are the planimetric components, r is the reference data (generated), and c, the ground truth (*check point*) in a given point i.
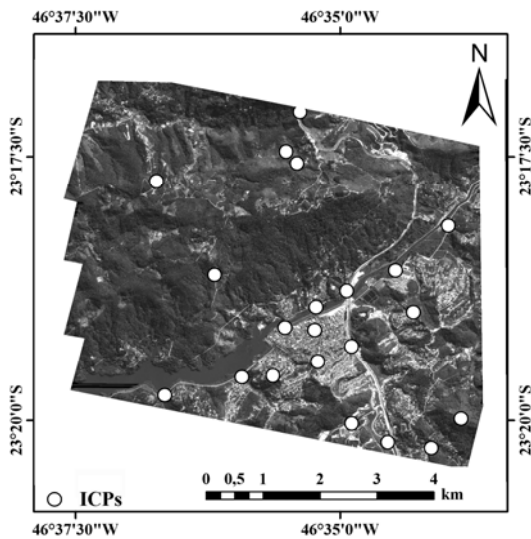

Fig. 5 - Location of the validation points.

The trend analysis and accuracy assessment were based on the methodology proposed by GALO & CAMARGO (1994) and comprises the following steps:

- calculation of mean (equation (5)) and standard deviation (equation (6)) of the samples discrepancies,

$$\hat{\mu} = \frac{1}{n} \sum_{i=1}^{n} \Delta h_i \quad, \tag{5}$$

$$\hat{\sigma} = \sqrt{\frac{1}{(n-1)} \sum_{i=1}^{n} (\Delta h_i - \hat{\mu})^2} \quad, \tag{6}$$

where Δh_i is the difference between the reference data and a given point i, and n is the number of samples (number of ICPs). The above equations are also used in the calculation of further discrepancies.

- calculation of the sample statistics t and its respective confidence interval. Through the *t-Student* test, it is possible to verify if the discrepancies mean is equal to zero and if trend or systematic shift is present in the data. In this test, the following hypotheses are evaluated:

$$H_0 : \hat{\mu} = 0 \text{, against} \tag{7}$$

$$H_1 : \hat{\mu} \neq 0. \tag{8}$$

In this test, the sample statistics t is calculated, and we verify if the value is contained within the interval for accepting or refusing the null hypothesis. The value of the t statistics is given by equation (9):

$$t_X = \frac{\hat{\mu}}{\hat{\sigma}} \sqrt{n} \quad, \tag{9}$$

and the decision rule used in order not to refuse the null hypothesis, by equation (10):

$$\left| t_x \right| < t_{(n-1, \alpha/2)} \quad, \tag{10}$$

where $\hat{\mu}$ corresponds to the discrepancies mean; $\hat{\sigma}$ is the sample standard deviation, and α accounts for the level of significance of the statistical test.

According to GALO & CAMARGO (1994), if the sample statistics t lies outside the confidence interval, the null hypothesis is rejected. That is to say, the cartographic product cannot be regarded as free of significant trends in the evaluated coordinate for the considered level of significance. In the cases when trend is observed, it is possible to correct it by subtracting its value in each coordinate of the DSM.

The accuracy assessment is accomplished with the chi-square test, where the standard deviation of the discrepancies is compared with the expected standard deviation for the desired class (Class A), considering the following hypotheses (ITAME, 2001):

$$H_0 : \hat{\sigma}^2 = \sigma^2 \text{, contra} \tag{11}$$

$$H_1 : \hat{\sigma}^2 > \sigma^2 \quad, \tag{12}$$

where σ is the expected standard deviation for the class of interest (Class A).

In face of the expected standard deviation value, the statistical analysis is carried out by the following equation (13):

$$\chi^2 = (n-1)\frac{\hat{\sigma}^2}{\sigma^2} \quad , \tag{13}$$

and we verify if the obtained value is contained within the acceptance interval, as follows (equation (14)):

$$\chi^2 \leq \chi^2_{(n-1;\alpha)} \quad . \tag{14}$$

If equation (11) is not met, we refuse the hypothesis H_0 which states that the cartographic product is up to standard (ITAME, 2001).

The root mean square error (RMSE) was calculated by equation (15):

$$RMSE = \sqrt{\frac{1}{n}\sum_{i=1}^{n}\Delta h_i^2} \quad . \tag{15}$$

When the mean of samples discrepancies is zero, the value of RMSE is equal to the standard error (SE), and thus, PEC is given by equation (16):

$$PEC = SE \; x \; 1,6449 \quad . \tag{16}$$

For the orthoimages, the trend analysis and accuracy assessment are executed in the same way, in which the elevation discrepancies are replaced by the positional discrepancies (ΔE_i and ΔN_i).

As previously explained, PEC is a cartographic accuracy measure used in Brazil. In positional terms, PEC is equivalent to the CE90, and with respect to elevation, PEC is equivalent to the LE90, both of them world-wide used. The PEC values used in this experiment are the ones related to scale 1: 10 000. The choice of this scale was based on a legal guideline that states the accuracy of a cartographic product corresponds to 1/3 of the standard error. According to a Brazilian Federal Decrete n. 89.817 (BRASIL, 1984), the positional standard error at a scale 1: 10 000 is 3 m. Therefore, the positional accuracy at this scale is 1 m, what exactly corresponds to the spatial resolution of the panchromatic band and the pan-sharpened multispectral bands of IKONOS images. Table 3 presents the elevation values of PEC and SE, and Table 4 presents the positional PEC and SE, all of them for Classes A, B, and C, according to Brasil (1984).

TABLE 3 - ELEVATION ACCURACY STANDARD AND STANDARD ERROR FOR CLASSES A, B, AND C (AS AN EQUIDISTANT FRACTION OF CONTOUR LINES).

CLASS	PEC (mm)	SE (mm)
A	1/2	1/3
B	3/5	2/5
C	3/4	1/2

TABLE 4 - POSITIONAL ACCURACY STANDARD AND STANDARD ERROR FOR CLASSES A, B, AND C.

CLASS	PEC (mm)	SE (mm)
A	0,5	0,3
B	0,8	0,5
C	1,0	0,6

4. RESULTS AND DISCUSSION

Based on the adopted models and the different GCPs settings, Table 5 presents the statistical evaluation results for the DSMs, and Table 6, the statistical evaluation results for the orthoimages.

Analysing the RPC modeling results, it is reasonable to state that the inclusion of GCPs reduces the RMSE. In this case, there was a significant improvement of 83.5% between the best DSM, obtained with 9 GCPs and with a RMSE of 1.03 m, and the relative DSM, with a RMSE of 1.89 m.

The difference between the RMSE values obtained for each absolute DSM generated with the RPC model was inferior to 9 cm. This small difference confirmed that the inclusion of more than 9 GCPs did not significantly improve the accuracy of the generated DSMs.

In the evaluation of the DSMs generated with Toutin´s model with no tie points, it could be observed that the best result was obtained with 9 GCPs, coinciding with the best result of the RPC model. When the RMSE values of the DSMs generated with this modelling approach are compared, it is noticeable that the difference between the best (DSM 2) and the worst result (DSMs 5 and 6) was inferior to 25 cm.

The adopted minimum number of GCPs (9) already presented an appropriate representativeness in terms of spatial distribution and elevation values, and hence, the inclusion of new GCPs did not reduce the RMSE values. On the contrary, the inclusion of GCPs decreased the DSMs generated with more than 9 GCPs.

In order to investigate the influence of tie points in the calculations of Toutin´s model, the 5 DSMs were again generated with the same amount of GCPs, but with the insertion of 11 tie points. The obtained results indicated that the best DSM was the one generated with 21 GCPs and 11 TPs (RMSE = 1.41 m). Comparing the results between the best and the worst value of RMSE, the difference was of 24 cm. This result demonstrates that the rigorous model is robust, and when GCPs and TPs are used, the RMSE values will be much better in comparison to the ones related to DSMs generated with no TPs.

Comparing the best results between the RPC and Toutin´s modelling approaches, the best DSM generated by the RPC model was the one with 9 GCPs (RMSE = 1.03 m), and the best DSM generated by

Toutin´s model was the one with 21 GCPs and 11 TPs (RMSE =1.41 m).

In the trend analyses, the DSMs generated by the two modelling approaches provided disagreeing results. In the case of the RPC model, only the relative DSM did not present trend. Regarding Toutin´s model with no TPs, the DSMs 2, 4, and 6 did not present trend, and in all DSMs with TPs, no trend was observed. As previously explained, the trend can be removed by subtracting its mean value from the Z component of each generated DSM.

In the accuracy analysis, all the DSMs generated either by the RPC or by Toutin´s model with TPs met the elevation *PEC* Class A at a scale 1:10000.

TABLE 5 - RESULTS OF THE TREND ANALYSIS AND ACCURACY ASSESSMENT FOR THE DSMs GENERATED WITH DIFFERENT GCPs SETTINGS.

	DSM 1	DSM 2	DSM 3	DSM 4	DSM 5	DSM 6
RPC Model						
GCPs	0	9	12	15	18	21
Standard Deviation	1.89	1.03	1.08	1.12	1.05	1.05
Mean	-0.56	-1.41	-1.63	-1.64	-1.67	-1.74
No Trend	true	false	false	false	false	false
Up to Accuracy Standard	yes	yes	yes	yes	yes	yes
RMSE	1.89	1.03	1.08	1.12	1.05	1.05
LE90	3.10	1.69	1.78	1.85	1.72	1.73
Toutin´s Model with no Tie Points						
GCPs	-------	9	12	15	18	21
Standard Deviation	-------	2.02	2.23	2.25	2.26	2.26
Mean	-------	0.38	1.05	0.82	0.88	0.68
No Trend	-------	true	false	true	false	true
Up to accuracy Standard	-------	no	no	no	no	no
RMSE	-------	2.02	2.23	2.25	2.26	2.26
LE90	-------	3.33	3.67	3.71	3.72	3.72
Toutin´s Model with Tie Points						
GCPs	-------	9	12	15	18	21
Standard Deviation	-------	1.56	1.50	1.50	1.65	1.41
Mean	-------	0.11	-0.10	0.13	0.20	-0.24
No Trend	-------	true	true	true	true	true
Up to Accuracy Standard	-------	yes	yes	yes	yes	yes
RMSE	-------	1.56	1.50	1.50	1.65	1.41
LE90	-------	2.56	2.47	2.47	2.71	2.33

TABLE 6 - RESULTS OF THE TREND ANALYSIS AND ACCURACY ASSESSMENT
FOR THE GENERATED ORTHOIMAGES.

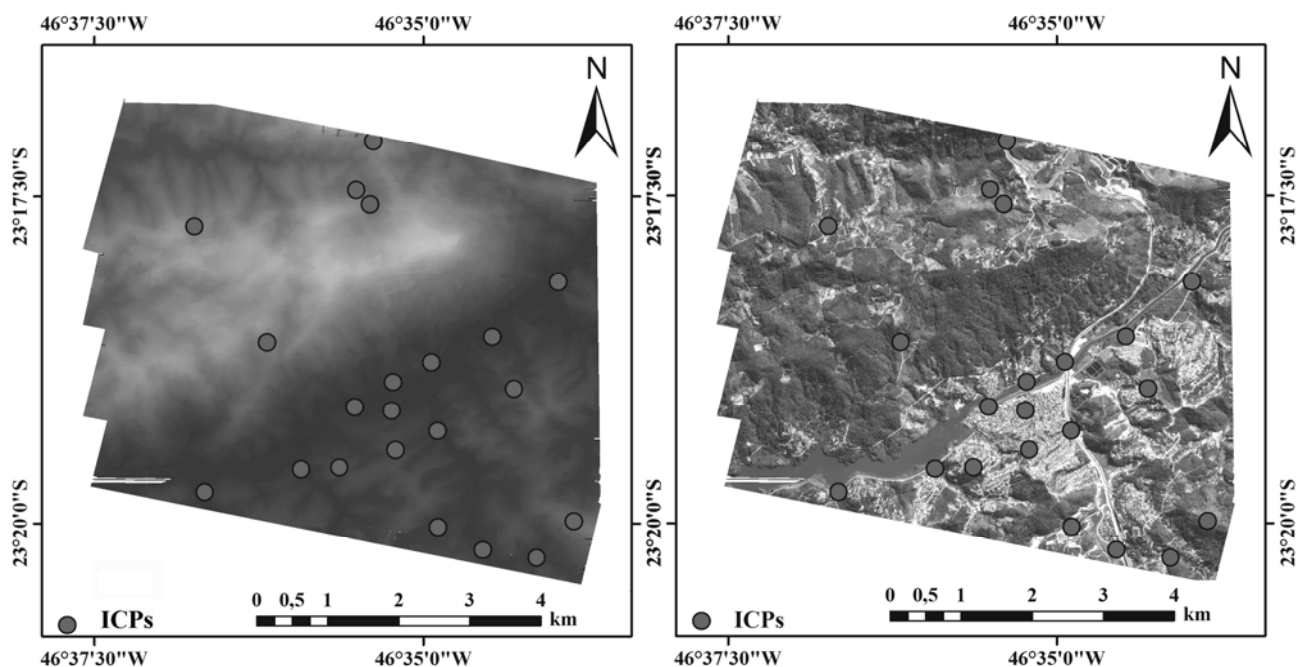|	Orthoimage 1 (RPC)			Orthoimage 2 (Toutin with TPs)		
	ΔE	ΔN	Resultante	ΔE	ΔN	Resultante
Standard Deviation	1.36	1.77	2.23	2.65	3.10	4,08
Mean	0.27	0.34	0.43	1.38	-0.02	1,38
RMSE	1.39	1.80	2.28	3.01	3.10	4,32
Trend Analysis						
t_x	0.93	0.87	0.89	2.39	0.03	1,56
$t_{(n-1;\ \alpha/2)}$	1.73	1.73	1.73	1.73	1.73	1,73
$|t_x| < t_{(n-1;\ \alpha/2)}$	true	true	true	false	true	true
Accuracy Analysis – Class A						
σ_x *(1:10.000 – Class A)*	2.12	2.12	2.12	2.12	2.12	2,12
χ^2_x	8.22	13.92	22.15	31.31	42.66	73,98
$\chi^2_{(n-1,\ \alpha)}$	28.41	28.41	28.41	28.41	28.41	28,41
$\chi^2_x \le \chi^2_{(n-1,\ \alpha)}$	true	true	true	false	false	false
Accuracy Analysis - Class B						
σ_x *(1:10.000 – Class B)*				3.54	3.54	3.54
χ^2_x				11.27	15.36	26.63
$\chi^2_{(n-1,\ \alpha)}$				28.41	28.41	28.41
$\chi^2_x \le \chi^2_{(n-1,\ \alpha)}$				true	true	true

Fig. 6 - Digital surface model (left) and orthoimage with the best accuracy (right),
both with the location of the 21ICPs.

Two orthoimages were generated from the best DSM obtained by each model – RPC and Toutin´s with TPs. The trend analysis and accuracy assessment results for both orthoimages are presented in Table 6.

For the first orthoimage, generated with 9 GCPs and using the DSM obtained by the RPC model, the trend and accuracy tests classified the product in Class A, scale 1:10 000. For the second orthoimage, generated with 21 GCPs and 11 TPs using the DSM obtained by Toutin´s model, it was observed a trend in the East component (E). When it is jointly analysed with the North component (N), which does not present trend, the resulting component of both is free of trend. Nevertheless, in the accuracy assessment analysis, this orthoimage was not up to Class A standards, and was hence assigned to Class B.

Likewise the elevation accuracy assessment, the orthoimage generated by the RPC model with 9 GCPs presented a superior result in relation to the one generated by Toutin´s model.

Figure 6 presents the DSM and the orthoimage with the best results (RPC model with 9 GCPs) as well as the ICPs used in the positional accuracy assessment of both of them.

The accuracy of DSMs and orthoimages depends on several factors, like the type of terrain (flat or steep), type of land use (urban or rural), size of the study area, adopted mathematical model, quality of GCPs etc. In the case of urban scenes, which present different kinds of features and elevations, it is common to occur oclusions and shadow, rendering it difficult to identify homologous features on the terrain, and hence, hindering the calculations of the mathematical model. In this way, it is possible to understand the controversies among the results found in the consulted literature, like in CHENG & TOUTIN (2001), DAVIS & WANG (2001), WOLNIEWICZ & JASZCZAK (2004), AGUILLAR *et al*. (2007), since they concern study areas with diverse characteristics.

In the work of CHENG & TOUTIN (2001), for instance, the DSM generated from an IKONOS stereo pair by the rigorous model, covering a semi-urban area to the North of Quebéc, Canada, presents elevation accuracies ranging from 4.6 m (best result) to 18 m (worst result), as a function of the type of land cover. Taking into account the entire study area, the LE90 was 7.9 m. The authors associated the best results to places with certain types of land cover, low elevation variation or flat areas; and the worst results to steep relief areas. Their results are not representative of DSMs generated from IKONOS stereo pairs in a generic way and must be solely considered for the study area analysed in their experiment.

Both the RPC model and Toutin´s model presented accuracy in the generation of DSMs. However, they are sensitive to the above mentioned factors. Therefore, for each study area it is expected that the models will present different behaviours. Our study area, located in the municipality of Mairiporã, presents steep relief, with elevation values ranging from 740 to 1,300 m, and diverse kinds of land cover, like urban areas, native vegetation, water bodies, etc. Consequently, the highest elevation error found in this experiment (RMSE = 2.26 m and LE90 = 3.72 m) is still in accordance with the average error values reported in the literature.

5. CONCLUSIONS

The RPC modelling approach presents some advantages in relation to Toutin´s approach, like a reduced dependence on the use of control points; possibility of generating a relative DSM (with no GCPs), and in the particular case of this work, results with higher accuracy. On the other hand, the DSMs generated with tie points using Toutin´s approach presented no trend.

In a general way, the inclusion of GCPs beyond the minimum amount required for each modelling approach did not significantly improve the DSMs accuracy. In this sense and considering that it is not always possible to collect ground control points in the field, it is advisable to strive for accuracy of such control points, both in their collection in the field and in their interpretation in the image.

Since the images are generally orthorectified by means of DSMs, and the latter ones are influenced by the terrain characteristics, type of land cover, and size of the study area, the orthoimages accuracy will be hence equally influenced by these factors.

REFERENCES

AGUILLAR, M. A.; AGUILAR, F. J.; CARVAJAL, F.; AGÜERA, F.; ESTRADA, L. Geometric accuracy of Ikonos Geo panchromatic orthoimage products. **ISPRS Commission I – Image Data Acquisition, Sensors and Platforms**, 2004 – 2008, Paris, França, ISPRS, 2007. Disponível em <http://isprs.free.fr/documents/Papers/PS1-07.pdf>. Acesso: 01 outubro 2009.

ARAÚJO, E. H. G.; KUX, H. J. H.; FLORENZANO, T. G. Ortorretificação de imagens do satélite quickbird para aplicações urbanas. **Revista Brasileira de Cartografia**, v. 60, n. 2, p. 205-213, 2008.

BALTSAVIAS, E.; PATERAKI, M.; ZHANG, L. Radiometric and geometric evaluation of Ikonos Geo

images and their use for 3D building modelling. In: Joint ISPRS Workshop "High Resolution Mapping from Space 2001", Hannover, Alemanha. **Proceedings**. Hannover, ISPRS, 2001.

BRASIL. **Decreto n. 89.817, de 20 de junho de 1984**. Dispõe sobre as instruções reguladoras das normas técnicas da cartografia nacional. Diário Oficial da República Federativa do Brasil, Brasília, 22 de junho de 1984.

BRITO, J.; COELHO, L. **Fotogrametria digital**. Instituto Militar de Engenharia, Rio de Janeiro, 2002. Disponível em <http:www.efoto.eng.uerj.br/ebook-pt.html>. Acesso: 16 setembro 2009.

BÜYÜKSALÍH, G.; KOÇAK, G.; ORUÇ, M.; AKÇIN, H.; JACOBSEN, K. Accuracy analysis, Dem generation and validation using russian TK-350 stereo-images. **The Photogrammetric Record**, v. 19, p. 200-218, 2004.

CAMARGO, F. F.; FLORENZANO, T. G.; ALMEIDA, C. M.; OLIVEIRA, C. G. Abordagens cognitivas para a identificação de unidades geomorfológicas por meio de dados ASTER/Terra. **Revista Brasileira de Geociências**, v. 39, p. 276-288, 2009.

CHENG, P. A.; GÓMEZ, F.; WEBER, M.; FLINGELLI, C. **Correcting the data: Mapping of IKONOS images using minimum ground controls**. PCIGeomatics, 2008. Disponível em <http://www.pcigeomatics.com/pdfs/Ikonos.pdf>. Acesso: 17 agosto 2009.

CHENG, P. A.; TOUTIN, T. Orthorectification and DEM generation from high resolution satellite data. In: 22nd Asian Conference on Remote Sensing (ACRS 2001), Singapura. **Proceedings**. Singapura: ISPRS, 2001. v. 2, p.1203–1208.

CHENG, P. A.; TOUTIN, T.; ZHANG, Y. QuickBird – Geometric correction, data fusion, and automatic DEM extraction. In: 24th Asian Conference on Remote Sensing (ACRS 2003), Pusan, Coréia do Sul. **Proceedings**. Pusan, ISPRS, 2003.

DAVIS, C. H.; WANG, X. Planimetric accuracy of Ikonos 1 m panchromatic orthoimage products and their utility for local government GIS basemap applications. **International Journal of Remote Sensing**, v. 24, p. 4267-4288, 2001.

DI, K.; MA, R.; LI, R. Geometric processing of Ikonos stereo imagery for coastal mapping applications. **Photogrammetric Engineering & Remote Sensing**, v. 69, p. 873-879, 2003.

DIAL, G. IKONOS satellite mapping accuracy. In: ASPRS Conference, 2000, Washington DC. **Proceedings**. Washington DC, Bethesda, American Society of Photogrammetry and Remote Sensing, 2000.

DIAL, G.; BOWEN, H.; GERLACH, F.; GRODECKI, J.; OLESZCZUK, R. IKONOS satellite, imagery, and products. **Remote Sensing of Environment**, v. 88, p. 23–36, 2003.

GALO, M.; CAMARGO, P. O. O uso do GPS no controle de qualidade de cartas. In: Congresso Brasileiro de Cadastro Técnico Multifinalitário (COBRAC-1994). Florianópolis, SC. **Anais**. Florianópolis, UFSC, 1994.

GRODECKI, J.; DIAL, G. Ikonos geometric accuracy. Space Imaging. In: Joint ISPRS Workshop "High Resolution Mapping from Space 2001", Hannover, Alemanha. **Proceedings**. Hannover, ISPRS, 2001.

HARRY, B.; HANLEY, I.; FRASER, C. S. Geopositioning accuracy of Ikonos imagery: Indications from two dimensional transformations. **The Photogrammetric Record**, v. 17, p. 317-329, 2008.

ITAME, O. Y. **Controle de qualidade aplicado na modelagem digital de terreno**. Dissertação de Mestrado em Ciências Cartográficas, Faculdade de Ciências e Tecnologia, Universidade Estadual Paulista, Presidente Prudente, 2001. 106p.

KYRIAKIDIS, P.; SHORTRIDGE, A. M.; GOODCHILD, M. Geostatistics for conflation and accuracy assessment of digital elevation models. **International Journal of Geographical Information Science**, v. 13, p. 677-707, 1999.

LABEN, C. A.; BROWER, B. V. **Process for enhancing the spatial resolution of multispectral imagery using pan-sharpening**. Technical Report, New Jersey, EUA, Eastman Kodak Company, 2000.

LI, R.; NIU, X.; LIU, C.; WU, B.; DESHPANDE, S. Impact of imaging geometry on 3D geopositioning accuracy of stereo Ikonos imagery. **Photogrammetric Engineering & Remote Sensing**, v. 75, p. 1119-1125, 2009.

MAUNE, D. F.; KOPP, S. M.; CRAWFORD, C. A.; ZERVAS, C. E. Introduction. In: MAUNE, D. F. (ed.). **Digital elevation model technologies and applications: the DEM users manual**. Bethesda, ASPRS, 2007. p. 1-34.

MERCHANT, D. C. Spatial accuracy standards for large scale line maps. **Technical Papers of the American Congress on Surveying and Mapping**, v. 1, p.222–231, 1982.

OGC. **The Open GIS Abstract Specification**, Topic 7, The Earth Imagery Case, 1999.

PARADELLA, W. R.; CECARELLI, I. C. F.; LUIZ, S.; OLIVEIRA, C. G.; OKIDA, R. Geração de carta topográfica com estéreo-pares *fine* do RADARSAT-1 e dados ETM+ LANDSAT 7 em ambiente de relevo montanhoso na Região Amazônica (Serra dos Carajás, Pará). **Revista Brasileira de Geociências**, v. 35, n. 3, p.323-332, 2005.

PEDRO, P. C.; ANTUNES, A. F. B.; MITISHITA, E. Ortorretificação de imagens de alta resolução utilizando os modelos APM (Affine Projection Model) e RPC (Rational Polynomial Coefficient). **Boletim de Ciências Geodésicas**, v. 13, p. 60-75, 2007.

TOUTIN, T. Error tracking in IKONOS geometric processing using a 3D parametric modeling. **Photogrammetric Engineering & Remote Sensing**, v. 69, p. 43-51, 2003.

TOUTIN, T. Comparison of stereo-extracted DTM from different high-resolution sensors: SPOT-5, EROS-a, IKONOS-II, and QuickBird. **IEEE Transactions on Geoscience and Remote Sensing**, v. 42, p. 2121-2129, 2004a.

TOUTIN, T. Review article: Geometric processing of remote sensing images: models, algorithms and methods. **International Journal of Remote Sensing**, v. 25, p. 1893-1924, 2004b.

TOUTIN, T. Comparison of 3D physical and empirical models for generating DSMs from stereo HR images. **Photogrammetric Engineering & Remote Sensing**, v. 72, p. 597-604, 2006.

TOUTIN, T.; CHENG, P. A. Demystification of IKONOS. **EOM**, July, p. 17-20, 2000.

VASSILOPOULOU, S.; HURNI, L.; DIETRICH, V.; BALTSAVIAS, E.; PATERAKI, M.; LAGIOS, E.; PARCHARIDIS, I. Orthophoto generation using IKONOS imagery and high-resolution DEM: a case study on volcanic hazard monitoring of Nisyros Island (Greece). **ISPRS Journal of Photogrammetry and Remote Sensing**, v. 57, p. 24-38, 2002.

WOLNIEWICZ, W.; JASZCZAK, P. Finding true position of buildings in orthophotos. In: 25th Asian Conference on Remote Sensing (ACRS 2004) & 1st Asian Space Conference, Chiang Mai, Tailândia. **Proceedings**. Chiang Mai, ISPRS, 2004.

YIMAZ, A.; OZERBIL, O. T.; EKER, O.; ERDOGAN, M.; MARAS, E. E. Investigation of 3D geopositioning and DEM accuracy of CARTOSAT-1 stereo imagery. In: ISPRS Congress Beijing 2008, Beijing, China. **Proceedings**. Beijing, ISPRS, 2008. v. 1, p.799-804.